Article

Amine-Assisted Facetted Etching of CdSe Nanocrystals

Rongfu Li, Jeunghoon Lee, Baocheng Yang, David N. Horspool, Mark Aindow, and Fotios Papadimitrakopoulos

J. Am. Chem. Soc., **2005**, 127 (8), 2524-2532• DOI: 10.1021/ja0465404 • Publication Date (Web): 03 February 2005

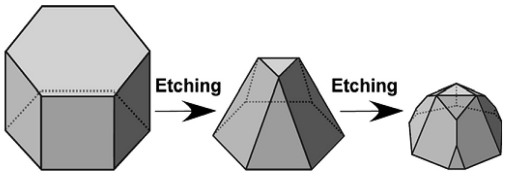

Evolution of CdSe NC morphology during etching in $HO(CH_2)_3NH_2$ / H_2O (v/v =10:1) at 80 ± 5° C

More About This Article

Additional resources and features associated with this article are available within the HTML version:

- Supporting Information
- Links to the 10 articles that cite this article, as of the time of this article download
- Access to high resolution figures
- Links to articles and content related to this article
- Copyright permission to reproduce figures and/or text from this article

View the Full Text HTML

J|A|C|S
ARTICLES
Published on Web 02/03/2005

Amine-Assisted Facetted Etching of CdSe Nanocrystals

Rongfu Li,[†] Jeunghoon Lee,[†] Baocheng Yang,[‡] David N. Horspool,[§] Mark Aindow,[§] and Fotios Papadimitrakopoulos*[,†,‡]

Contribution from the Nanomaterials Optoelectronics Laboratory, Polymer Program, Department of Chemistry, and Department of Metallurgy and Materials Engineering, Institute of Materials Science, University of Connecticut, Storrs, Connecticut 06269

Received June 11, 2004; E-mail: papadim@mail.ims.uconn.edu

Abstract: The treatment of CdSe nanocrystals (NCs) in a 3-amino-1-propanol (APOL)/water (v/v = 10:1) mixture at 80 °C in the presence of O_2 causes them to undergo a slow chemical etching process, as evidenced by spectroscopic and structural investigations. Instead of the continuous blue shift expected from a gradual decrease in NC dimensions, a bottleneck behavior was observed with distinct plateaus in the peak position of photoluminescence (PL) and corresponding maxima in PL quantum yield (i.e., 34 ± 7%). It is presently argued that such etching behavior is a result of two competitive processes taking place on the surface of these CdSe NCs: (i) oxidation of the exposed Se-sites to acidic SeO_x entities, which are readily solubilized in the basic APOL/H_2O mixture, and (ii) coordination of the underlying Cd-sites with both amines and hydroxyl moieties to temporally impede NC dissolution. This is consistent with the HRTEM results, which suggest that the etched NCs adopt pyramidal morphologies with Cd-terminated facets (i.e., (0001) bases and either $\{01\bar{1}1\}$ or $\{2\bar{1}\bar{1}1\}$ sides) and account for the apparent resistance to etching at the plateau regions.

Introduction

CdSe-based quantum-confined systems have attracted significant interest from the scientific community in recent years.[1,2] This interest originated from the successful synthesis of fairly monodisperse CdSe NCs (<5% rms in diameter) by employing the pyrolysis of organometallic precursors within thermally stable amphiphiles.[3,4] Since then, various synthetic modifications have been introduced in order to have better control of size, size distribution[5−11] and shape (i.e. dots,[4] rods,[5,7,8] teardrops,[12] etc.) that greatly expanded the architectural flexibility of CdSe NCs. This flexibility enabled CdSe NCs to find a variety of applications such as electronic and photonic applications (i.e, lasing,[13] light emitting diodes (LEDs),[1,2] and nonlinear optics[14,15]) as well as biolabeling/biotagging agents.[16−18]

For NC diameters smaller than their bulk exciton Bohr radius,[4,19] quantum confinement is manifested by the blue shift of both UV/vis absorption and PL emission as their size decreases. To improve the PL efficiency of CdSe NCs, considerable efforts have been exerted on obtaining adequate passivation of various surface states, acting as traps that reduce exciton radiative recombination.[2] Core/shell structures, where a higher band gap inorganic material (i.e., ZnS[20,21] or CdS,[22] etc.) has been used to clad the CdSe core, have been shown to provide adequate passivation. This passivation however is feasible only for a few monolayers of cladding materials, since the underlying lattice mismatch between the core and the higher band gap overcoating semiconductor severely diminish performance as cladding thickness increases.[21] This has prompted researchers to investigate more carefully organic passivation layers that are expected to be more tolerant in terms of lattice mismatch. Amphiphiles such as trioctylphosphine oxide (TOPO)/trioctylphosphine (TOP),[1,4] alkylamines,[23] pyridine,[1,4,23] thiols, and dithiols[17,24] have been investigated as CdSe capping agents.

[†] Polymer Program
[‡] Department of Chemistry
[§] Department of Metallurgy and Materials Engineering

(1) Murray, C. B.; Kagan, C. R.; Bawendi, M. G. *Annu. Rev. Mater. Sci.* **2000**, *30*, 545−610.
(2) Alivisatos, A. P. *J. Phys. Chem.* **1996**, *100*, 13226−13239.
(3) Nirmal, M.; Murray, C. B.; Norris, D. J.; Bawendi, M. G. *Z. Phys. D: At., Mol. Clusters* **1993**, *26*, 361−363.
(4) Murray, C. B.; Norris, D. J.; Bawendi, M. G. *J. Am. Chem. Soc.* **1993**, *115*, 8706−8715.
(5) Peng, X. G.; Manna, L.; Yang, W. D.; Wickham, J.; Scher, E.; Kadavanich, A.; Alivisatos, A. P. *Nature* **2000**, *404*, 59−61.
(6) Peng, Z. A.; Peng, X. *J. Am. Chem. Soc.* **2001**, *123*, 183−184.
(7) Peng, Z. A.; Peng, X. *J. Am. Chem. Soc.* **2002**, *124*, 3343−3353.
(8) Peng, Z. A.; Peng, X. *J. Am. Chem. Soc.* **2001**, *123*, 1389−1395.
(9) Qu, L.; Peng, X. *J. Am. Chem. Soc.* **2002**, *124*, 2049−2055.
(10) Qu, L.; Peng, Z. A.; Peng, X. *Nano Lett.* **2001**, *1*, 333−337.
(11) Peng, X.; Wickham, J.; Alivisatos, A. P. *J. Am. Chem. Soc.* **1998**, *120*, 5343−5344.
(12) Manna, L.; Milliron, D. J.; Meisel, A.; Scher, E. C.; Alivisatos, A. P. *Nat. Mater.* **2003**, *2*, 382−385.
(13) Klimov, V. I.; Mikhailovsky, A. A.; Xu, S.; Malko, A.; Hollingsworth, J. A.; Leatherdale, C. A.; Eisler, H.-J.; Bawendi, M. G. *Science* **2000**, *290*, 314−317.
(14) Ispasoiu, R. G.; Jin, Y.; Lee, J.; Papadimitrakopoulos, F.; Goodson, T., III. *Nano Lett.* **2002**, *2*, 127−130.
(15) Ispasoiu, R. G.; Lee, J.; Papadimitrakopoulos, F.; Goodson, T., III. *Chem. Phys. Lett.* **2001**, *340*, 7−12.
(16) Chan, W. C. W.; Maxwell, D. J.; Gao, X.; Bailey, R. E.; Han, M.; Nie, S. *Curr. Opin. Biotechnol.* **2002**, *13*, 40−46.
(17) Chan, W. C. W.; Nie, S. *Science* **1998**, *281*, 2016.
(18) Han, M.; Gao, X.; Su, J. Z.; Nie, S. *Nat. Biotechnol.* **2001**, *19*, 631−635.
(19) Brus, L. *J. Phys. Chem.* **1986**, *90*, 2555−2560.
(20) Dabbousi, B. O.; Rodriguez-Viejo, J.; Mikulec, F. V.; Heine, J. R.; Mattoussi, H.; Ober, R.; Jensen, K. F.; Bawendi, M. G. *J. Phys. Chem. B* **1997**, *101*, 9463−9475.
(21) Hines, M. A.; Guyot-Sionnest, P. *J. Phys. Chem.* **1996**, *100*, 468−471.
(22) Peng, X.; Schlamp, M. C.; Kadavanich, A. V.; Alivisatos, A. P. *J. Am. Chem. Soc.* **1997**, *119*, 7019−7029.

10.1021/ja0465404 CCC: $30.25

Among various organic amphiphiles used to passivate CdSe NCs, alkylamines have recently attracted attention due to their ability to organize on nanosized surface of CdSe NCs.[25] In the absence of O_2, these amines are thermally stable and have been used as coordinating agents in the synthesis of CdSe NCs.[7,9,23] Talapin et al.[23] have shown that upon exchanging the TOPO/TOP capping agents with allylamine at 50 °C, or dodecylamine at 100 °C, a significant improvement in band-edge PL quantum yield of the CdSe NCs has been observed. This report, however, is in contrast to that of Landes et al.[26] that the PL of CdSe NCs was quenched by the presence of amines. These apparently contradictory results are further complicated by the observation of large absorption blue shift for small CdSe NCs in the presence of amines.[27] Interestingly, as it will be argued in this paper, such quenching or enhancement phenomena might originate from amine-assisted chemical etching of CdSe NCs.

In this contribution we report a controlled, O_2-assisted etching of CdSe NCs by heating them at 80 ± 5 °C in 10/1 (3-amino-1-propanol (APOL))/water mixtures. This etching process is governed by two competitive processes: (i) Surface-exposed Se sites are oxidized into acidic SeO_x moieties, which are readily solubilized in the basic medium rendering the exposure of the underlying Cd sites. (ii) The coordination of basic amine and hydroxyl moieties to cadmium terminated NC surfaces temporally impede solubilization of the Cd sites and thereby prevent further exposure of the underlying Se sites. These manifest to discrete plateaus in the etching behavior of these CdSe NCs, as witnessed from both UV−vis and PL measurements. High-resolution TEM analysis indicates that these NCs adopt pyramidal morphologies consistent with Cd-terminated polar facets. Moreover, as suggested by the photoluminescence QY maxima and fwhm emission minima in the plateau regions, this "bottleneck" type of etching could provide a possible venue for reconstruction and surface modification of CdSe NCs.

Experimental Section

Chemicals: Trioctylphosphine (TOP) 90%, trioctylphosphine oxide (TOPO) 90%, and 3-amino-1-propanol (APOL) 99% (water content, <0.4%) were purchased from Aldrich. Selenium shots 99.999% were purchased from Alfa, and dimethylcadmium 97% was purchased from Strem. Absolute methanol, ethanol, and chloroform were purchased from J.T. Baker. Methyl sulfoxide-d_6 (DMSO-d_6) 99.9% atom D and chloroform-*d* ($CDCl_3$) 99.8% atom D were purchased from Acros organics. All chemicals were used as received, unless otherwise stated.

Synthesis of CdSe Nanocrystals: CdSe nanocrystal samples were synthesized based on the high-temperature pyrolysis of organometallic precursors[3,4,11,22] with minor modification. For example, 30 g of technical grade TOPO was degassed under dynamic vacuum at ~150 °C for 4 h in a reaction vessel equipped with a condenser, thermometer, and rubber septum. Consequently the reaction vessel was filled with nitrogen, and the temperature was raised to 300 °C. Selenium (0.3 g) was dissolved in 15 mL of TOP in inert atmosphere. After the selenium was completely dissolved, 0.35 mL of dimethylcadmium was added, and the mixture was loaded into a syringe followed by a quick injection into the reaction vessel with hot TOPO (while the heating mantle was temporarily removed). This causes the temperature of the reaction mixture to rapidly drop to ~200 °C and a characteristic color change to take place due to the formation of CdSe NCs. The heating was then restored and allowed the mixture's temperature to be raised between 260 and 300 °C permitting the NCs to grow to the desired size (as determined by UV−vis absorption). The solution was then cannulated out of the reaction vessel, and 100 mL of methanol were added to induce NC precipitation. The precipitate was collected by centrifugation and washed in triplicate with methanol.

Etching of CdSe Nanocrystals: Precipitated TOPO/TOP capped CdSe NCs were exchanged with APOL to form a clear solution that was then precipitated by acetone to remove both TOPO and TOP. The NC precipitate was then redispersed in APOL and stirred for a few hours until a clear stock solution was obtained. The optical density (OD) of the stock and other concentrated solutions were obtained by measuring the OD of diluted mixtures to ensure that the resulting solution had an OD value well below 1. Similarly, the same stock solution was diluted by APOL and H_2O (v/v = 10/1) to yield sample A and B having 3.0 and 1.5 optical densities (OD), respectively, with respect to their first electronic absorption peak (~560 nm). CdSe NCs with 3.0 OD at the first electronic absorption peak dispersed in APOL only were also prepared to elucidate the effect of water on the etching process. These solutions were further immersed into a deeply colored oil bath at a temperature of 80° ± 5 °C, which excluded nearly all-optical radiation from the ambient yellow-lit room from reaching the NC solutions. Aliquots of 100 μL were collected at regular intervals, diluted by ethanol to 3 mL, and followed by collecting their UV−vis absorption and photoluminescence (PL) spectra.

Determining the Effect of Dissolved Oxygen on the Etching Process: A CdSe NC APOL/H_2O (v/v = 10/1) solution with 3.0 OD at its first electronic absorption peak (~560 nm) was placed into six glass tubes and sealed under vacuum separately after several (exceeding five) freeze−pump−thaw cycles. These sealed tubes were immersed into a dark oil bath heated at 80 ± 5 °C. At regular intervals, individual tubes were taken out from the oil bath, and their UV−vis absorption and PL emission were measured.

Determination of the Cd^{2+} Ionic Strength on the Etching Process: Anhydrous $CdCl_2$ (1.84 g, 0.01 mol) was dissolved in 10 mL of H_2O to obtain a 1 M $CdCl_2$ solution. This solution was then diluted with water to render a series of $CdCl_2$ solutions with concentrations of 0.5, 0.1, 0.05, and 0.01 M, respectively. These solutions were added to the CdSe NC solution in APOL to render solutions of different Cd^{2+} concentrations, yet maintaining the same ratio of APOL to water (i.e., v/v = 10:1) and same initial concentration of CdSe NCs (i.e., OD of 0.15 at 560 nm). These solutions were then subjected to similar annealing conditions (80 ± 5 °C) described above, and the evolution of CdSe NCs' optical properties was monitored by their UV−vis and PL spectra.

HRTEM Sample Preparation: To investigate the size and surface morphology changes of CdSe NCs during the etching process, CdSe NCs (with first electronic absorption peak at 625 nm) were etched under the same conditions mentioned above (in APOL/H_2O (v/v = 10:1) at 80 ± 5 °C) for various times. When the photoluminescence of this sample reached red (ca. 600 nm) at ~24 h and green (ca. 525 nm) at ~2 weeks, a small amount was withdrawn from the etching solution and a TOPO/TOP/*n*-octylamine (10%/20%/70 wt %) was added and allowed to mix for 10 min before inducing precipitation by the addition of methanol. As before, the excess of surfactants (i.e. APOL, TOPO, TOP, and *n*-octylamine) was removed by extensive washing with methanol and the NC precipitate was then dissolved in chloroform to form a clear solution. Microdroplets of this solution were deposited onto ultrathin (ca. 10 nm) carbon-coated TEM grids for examination by high-resolution TEM (HRTEM).

Characterization Methods: The room temperature UV−vis absorption spectra and steady-state photoluminescence of CdSe NC

(23) Talapin, D. V.; Rogach, A. L.; Kornowski, A.; Haase, M.; Weller, H. *Nano Lett.* **2001**, *1*, 207−211.
(24) Mattoussi, H.; Mauro, J. M.; Goldman, E. R.; Anderson, G. P.; Sundar, V. C.; Mikulec, F. V.; Bawendi, M. G. *J. Am. Chem. Soc.* **2000**, *122*, 12142−12150.
(25) Meulenberg, R. W.; Strouse, G. F. *J. Phys. Chem. B* **2001**, *105*, 7438−7445.
(26) Landes, C.; Burda, C.; Braun, M.; El-Sayed, M. A. *J. Phys. Chem. B* **2001**, *105*, 2981−2986.
(27) Landes, C.; Braun, M.; Burda, C.; El-Sayed, M. A. *Nano Lett.* **2001**, *1*, 667−670.

solution were obtained from a Perkin-Elmer LAMDA-900 UV−NIR spectrometer and a Perkin-Elmer LS50B fluorometer, respectively. PL quantum yields were obtained according to reported procedures,[4,9] using coumarin 485 and rhodamine 6G as standards with QY of 21% and 95%, respectively. The size, size distribution, structure, and orientation of the CdSe NCs were analyzed by HRTEM in a JEOL 2010 FasTEM operating at 200 kV. The HRTEM was equipped with a high-resolution objective lens pole-piece (spherical aberration coefficient Cs = 0.5 mm) providing a point-to-point resolution of <0.19 nm in phase contrast images. The TEM specimens were prepared by depositing a dilute chloroform solution of TOPO/TOP/*n*-octylamine capped CdSe NCs onto an ultrathin (~10 nm) amorphous carbon substrate supported on a copper mesh grid.

Results and Discussion

Synthesis of CdSe nanocrystals (NCs) by high temperature pyrolysis of organometallic precursors generally results in a hexagonal (wurtzite) crystalline structure, with well-defined morphology and relatively narrow size distribution.[4] The photoluminescence (PL) properties of the CdSe NCs are very much dependent on both the surface termination and the presence of various surface passivation agents.[2] By exchanging the TOPO/TOP surfactants with alkylamines, higher PL quantum yields (QYs) have been reported.[23] To promote NC solubility in polar media (i.e., alcohols and mixtures of alcohol with H_2O), a similar exchange of TOPO/TOP surfactant was performed with amino alcohols instead of *n*-alkylamines. This was accomplished by precipitating and washing the NCs with methanol, followed by their dispersion in neat 3-amino-1-propanol (APOL). Ethanolic solution of the APOL-capped CdSe NCs were further precipitated in acetone and redispersed in APOL or APOL/H_2O (v/v = 10/1) mixtures to ensure complete removal of the initial TOPO and TOP surfactants (see Supporting Information Figures S1 and S2). Unlike the TOPO/TOP passivated CdSe NC solutions that are stable over long period of time, APOL stabilized NCs exhibited a gradual blue shift in both their UV−vis absorption and luminescent properties. This gradual blue shift was found to accelerate with increasing temperature. In this contribution, a careful investigation of this phenomenon was performed by annealing CdSe NCs (1.84 g, 0.01 mol) at 80 ± 5 °C in APOL and APOL/H_2O (v/v = 10/1) mixtures. This temperature was found to be ideal for accelerating this process, yet avoiding the gradual discoloration of APOL in the presence of dissolved oxygen. As will be shown below, the concentration of oxygen in APOL or APOL/H_2O (v/v = 10/1) mixtures is of key importance to this process. Moreover, the concentration of oxygen cannot be increased beyond that of its ambient solubility in APOL (ca. 5 ppm[28]); otherwise APOL discolors even upon heating at 80 ± 5 °C. Based on this, the concentration of CdSe NCs was varied experimentally to adjust the NC-to-O_2 ratio, assuming that the solubility of oxygen in APOL is constant. In this experiment, CdSe NC solutions with two different concentrations were prepared by adjusting the optical density (OD) of their first electronic transition (ca. 560 nm) to 3.0 (sample A) and 1.5 (sample B), respectively. Annealing experiments for both samples A and B were carried out in parallel to keep all the other experimental factors the same. At regular intervals aliquots of 100 μL were withdrawn from each of these two etching solutions and diluted with 3.00 mL of ethanol, and their UV−vis and PL spectra were sequentially collected. Ambient light was carefully excluded during both annealing and sample dilution stages to avoid interference from the well-known photooxidation-induced etching of CdSe NC.[29−31]

Figure 1a and b illustrate the evolution of the UV−vis absorption (a) and PL emission (b) upon heating CdSe NCs of sample A (3.0 OD) in APOL/H_2O (v/v = 10/1) mixtures at 80 ± 5 °C. Similar trends were observed with the more dilute sample B (1.5 OD) (shown in Figure 1c and d). The apparent blue shift of the first electronic absorption in their UV−vis spectra, along with the more stepwise blue shift of their corresponding PL spectra, is consistent with the gradual etching of these CdSe NCs. For the sake of clarity, the evolution of both UV−vis and PL spectra during this etching experiment has been divided into four distinct regimes as shown in Figure 1. In regime I, which corresponds to annealing for up to 23 and 8 h for samples A and B, respectively, the wavelength positions of both the first electronic absorption (~560 nm) and the corresponding PL peak position (~580 nm) do not show any noticeable changes. However, the PL intensity at 580 nm increases to a maximum during the first 3 h of annealing and then decreases monotonically. The highest PL quantum yield obtained at this peak is ~37 ± 7% for samples A and B, when compared with rhodamine 6G as a standard.[4,10] It is interesting to note that, within experimental error, the PL quantum yield is independent of the concentration of CdSe NCs. In regime II, which corresponds to annealing for 23−46 and 8−27 h for samples A and B, respectively, considerable broadening and blue shifting is witnessed at the absorption edge of these NCs. This broadening was accompanied by a substantially weaker and broader PL emission, which is also blue shifted compared to that of regime I. In regime III, spanning from 46 to 92 h for sample A and 27−51 h for sample B, the first electronic absorption peak narrows again at ca. 480 nm. Similarly, the PL emission narrows at 495 nm and is also accompanied by a substantial increase in its intensity. Furthermore, the PL intensity in regime III gradually increases, then plateaus, and finally decreases monotonically, in a fashion similar to that of regime I, although the duration for this cycling was much shorter in regime I than in regime III. The highest PL quantum yield at 495 nm in this etching regime is ~32 ± 7% for sample A and 29 ± 7% for sample B, based on coumarin 485 as a standard.[4,10] In regime IV, which corresponds to annealing for 92−117 and 51−66 h for samples A and B, respectively, the 480 nm electronic absorption in the UV−vis spectra and the corresponding 495 nm PL emission gradually broaden and disappear, consistent with the gradual etching away of the CdSe NCs.

To provide a clearer picture of this etching process, the peak position (λ_{max}), QY, and the full width at half-maximum (fwhm) of the PL spectra for both sample A and sample B are plotted in Figure 2 as a function of annealing time, along with the four distinct regimes discussed above. The λ_{max}'s for both samples exhibit plateaus at 580 and 495 nm for regimes I and III, respectively. These plateaus are clearly associated with maxima

(28) Rooney, P. C.; Daniels, D. D. *Petroleum Technology Quarterly* **1998**, *Spring* 97−101.

(29) Katari, J. E. B.; Colvin, V. L.; Alivisatos, A. P. *J. Phys. Chem.* **1994**, *98*, 4109−4117.

(30) van Sark, W. G. J. H. M.; Frederix, P. L. T. M.; Van den Heuvel, D. J.; Gerritsen, H. C.; Bol, A. A.; van Lingen, J. N. J.; de Donega, C.; Meijerink, A. *J. Phys. Chem. B* **2001**, *105*, 8281−8284.

(31) Zhang, C.; O'Brien, S.; Balogh, L. *Abstracts of Papers, 223rd ACS National Meeting, Orlando, FL, United States, April 7−11, 2002*; COLL-305.

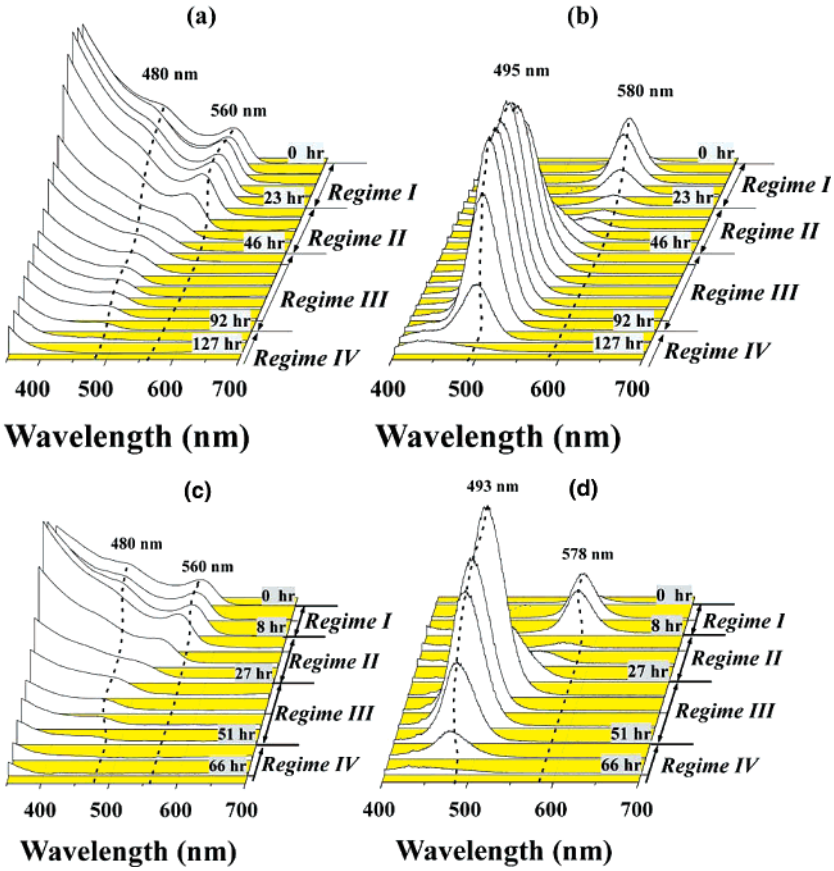

Figure 1. Evolution of (a and c) UV/vis absorption and (b and d) PL emission upon annealing CdSe nanocrystals of samples A (a and b, 3.0 OD) and B (c and d, 1.5 OD) in an APOL/H_2O (v/v = 10/1) mixture at 80 ± 5 °C for the indicated duration (380 nm PL excitation).

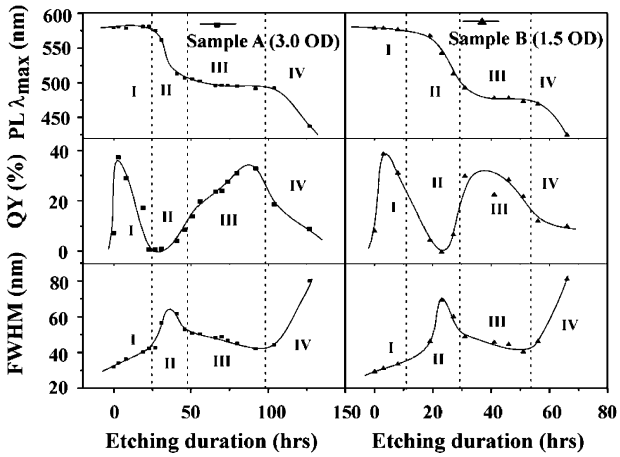

Figure 2. Evolution of PL peak position (λ_{max}), quantum yield (QY), and full width at half-maximum (fwhm) of CdSe NCs of samples A (3.0 OD) and B (1.5 OD) shown in Figure 1.

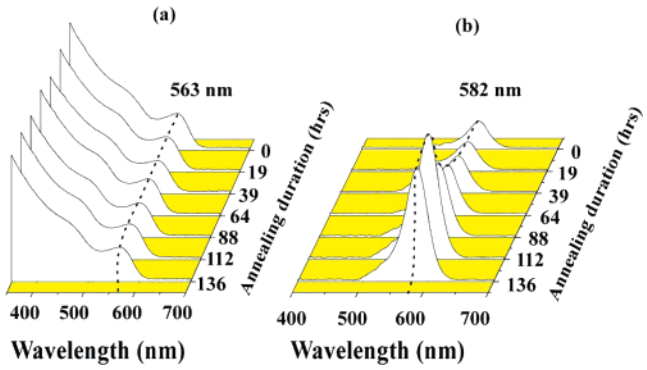

Figure 3. Evolution of (a) UV/vis absorption and (b) PL emission upon annealing CdSe nanocrystals (3.0 OD) in an oxygen-free APOL/H_2O (v/v = 10:1) at 80 ± 5 °C (380 nm PL excitation).

in PL quantum yield and minima in the fwhm graphs for both samples A and B. On the other hand, the transient λ_{max}'s in regimes II and IV exhibit the inverse type of behavior with that of regimes I and III, i.e., minima in PL quantum yield and maxima in fwhm for both samples A and B, respectively. These observations are reminiscent of similar trends observed in the synthesis of CdSe QDs where the term "focusing" has been associated with the narrowing of the size distribution, while "defocusing" implies the inverse behavior.[11] Using this terminology one might attempt to describe regimes I and III as "focusing" stages in the etching process, while regimes II and IV represent the "defocusing" stages that lead to the next stable NC size.

In an effort to elucidate the various parameters that influence this etching process, the role of dissolved oxygen in the APOL/H_2O solution was determined by thorough sample degassing. This was accomplished by subjecting the APOL/H_2O solution of CdSe NCs to multiple freeze−pump−thaw cycles under high vacuum (ca. 10^{-5} Torr), followed by sealing under vacuum into ampules to prevent reintroduction of O_2 during thermal annealing at 80 ± 5 °C. Similar to Figure 1, Figure 3 presents the UV−vis absorption and PL emission of these CdSe NC solutions as a function of annealing duration at 80 ± 5 °C. The profound absence of blue shifting transitions for either their electronic

absorption or PL emission indicates that these CdSe NCs are stable in APOL/H_2O (v/v = 10/1) mixtures when oxygen is not present. Interestingly enough, although the UV absorption spectra did not show any appreciable changes, the same was not true for the PL of these CdSe NCs. After annealing in excess of 64 h at 80 ± 5 °C, a gradual increase in the PL intensity of these NCs was observed along with the sharpening of their emission peak. This might be indicative of a possible surface reconstruction when etching is arrested.

The Se sites on the CdSe NC surface are expected to be particularly susceptible toward oxidation into selenium oxide, as previously reported from numerous photo-oxidation studies.[29−31] Katari et al. have shown that, upon exposure of CdSe NCs to air, the selenium surface sites were oxidized to SeO_2.[29] Such oxidative processes have also been linked to blue shifting in photoluminescence indicative that SeO_x species might act as a higher band gap material that contributes to greater quantum confinement in these CdSe NCs.[30] Unlike photo-oxidation, however, where light provides sufficient activation energy, thermally assisted oxidation relies only on the small amount of energetically active collisions to overcome the activation barrier associated with such a process. Moreover, the acidic nature of the surface generated selenium oxide species renders them highly soluble in the basic APOL/H_2O environment. The following chemical reactions depict few of the many possible reaction pathways that could be at play for such a complex system.

$$CdSe + 3/2\,O_2 \xrightarrow{\triangle} CdO + SeO_2 \quad \cdots\cdots (1)$$

$$SeO_2 + H_2O + 2\,HO\text{-}(CH_2)_3\text{-}NH_2 \rightleftharpoons [HO\text{-}(CH_2)_3\text{-}\overset{+}{N}H_3]_2\,SeO_3^{2-} \quad \cdots\cdots (2)$$

$$CdO + 2\,HO\text{-}(CH_2)_3\text{-}NH_2 + [HO\text{-}(CH_2)_3\text{-}\overset{+}{N}H_3]_2\,SeO_3^{2-} \rightleftharpoons [Cd(NH_2\text{-}(CH_2)_3\text{-}OH)_4]^{2+}SeO_3^{2-} + H_2O \quad \cdots (3)$$

Reactions 2 and 3 facilitate the dissolution of SeO_2 and CdO oxidation byproducts (eq 1) in APOL/H_2O mixtures, respectively, thereby accounting for the observed etching behavior of CdSe NCs in APOL.

The systematic investigation of all variables in this thermal oxidation process is challenged by a number of experimental difficulties associated with the peculiarities of this system. For example, one would like to study the effect of oxygen and/or SeO_2 concentration to the kinetics of thermal oxidation and the respective NC etching. Unfortunately the range of oxygen and SeO_2 concentration that such etching is meaningful is severely limited by the oxidative instability of APOL itself at high enough O_2 and SeO_2[32] concentration. To circumvent such oxygen sensitivity, our experiment was conducted with two different concentrations of CdSe NCs (with starting optical densities (OD) at 560 nm of 3.0 and 1.5, respectively), while keeping the amount of oxygen steady to the dissolved equilibrium concentration at 80 ± 5 °C (which is below 5 ppm[28]), thus varying the relative NC-to-O_2 concentration. As shown in Figure 2, the NC sample with an OD of 1.5 at 560 nm has a higher etching rate due to the higher O_2-to-CdSe NC ratio.[33]

The influence of water was then investigated by performing etching experiments in neat APOL at similar experimental conditions as those before (in the presence of dissolved O_2). Figure 4 depicts the evolution of UV/vis absorption (a) and PL emission (b) for APOL dispersed CdSe NCs as a function of annealing time in the absence of 10% H_2O. Similar to Figure 1, the discrete blue shifting transitions observed for both the electronic absorption and fluorescence emission of these NCs are in accordance with the stepwise etching behavior observed in oxygenated APOL/H_2O (v/v = 10/1) mixtures. However, the etching rates of CdSe NCs in neat APOL are nearly double that of CdSe NCs within APOL/H_2O (v/v = 10/1) mixtures. Figure 5 summarizes the evolution of peak position, QY, and fwhm of the PL emission for CdSe NCs etched in neat APOL. When these results are compared to those of Figure 2, it becomes apparent that the absence of a significant amount of water not only influences the etching rate but also negatively impacts the surface reconstruction of these etched NCs. With the exception of the 4 h data point, which shows a PL quantum yield on the order of 12%, all remaining measurements lay below 5% efficiency, as opposed to 34 ± 7% when about 10% H_2O is present. This might suggest that the formation of cadmium oxide (and corresponding hydroxides) on the CdSe NCs surfaces in

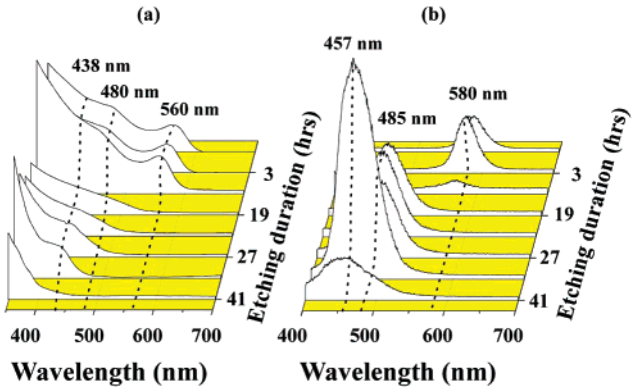

Figure 4. Evolution of (a) UV/vis absorption and (b) PL emission upon annealing CdSe nanocrystals (3.0 OD) in neat APOL at 80 ± 5 °C for indicated duration (380 nm PL excitation).

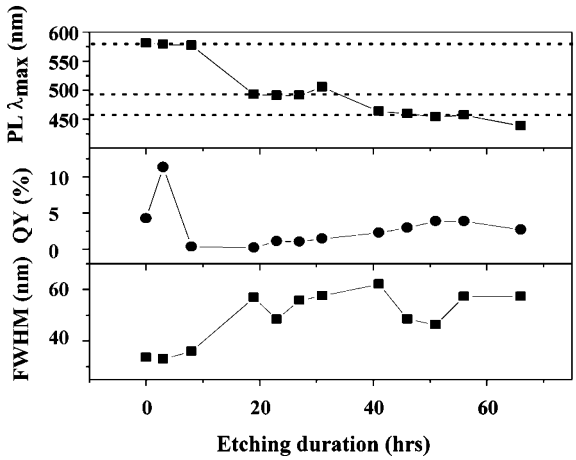

Figure 5. Evolution of PL peak position (λ_{max}), quantum yield (QY), and full width at half-maximum (fwhm) of the emission spectra of CdSe NCs (3.0 OD) etched in neat APOL as a function of etching time.

(32) Hoon Sik, K.; Yong Jin, K.; Hyunjoo, L.; Sang Deuk, L.; Chong Shik, C. *J. Catalysis* **1999**, *184*, 526−534.

(33) The etching rate is defined as the inverse of the etching duration. The etching duration is the total time for the CdSe NC samples being completely etched away. This is signified by the disappearance of the excitonic absorbance and corresponding PL emission.

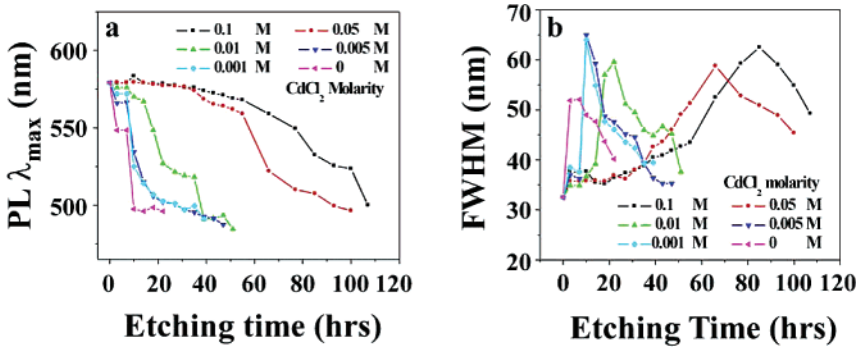

Figure 6. Evolution of PL peak position (λ_{max}) and full width at half-maximum (fwhm) of the CdSe NC (OD 0.15) in the presence of various concentrations of $CdCl_2$ during etching in APOL/H_2O (v/v = 10/1) mixtures at 80 ± 5 °C (380 nm PL excitation).

the presence of water not only increases the PL quantum yield at the plateau regimes but also enhances NC stability against further etching.

The results discussed above, are analogous to prior reports indicating an increase in PL quantum efficiency upon treating CdS NCs in the alkaline solution, attributed to the formation of surface passivating cadmium hydroxide species.[34,35] The alkaline nature of the etching medium APOL/H_2O should also help to form a cadmium oxide/hydroxide monolayer on the CdSe NC surface. However, in the neat APOL, this cadmium oxide species cannot be formed due to the lack of water. With 10% H_2O in the etching medium, the etching rate for CdSe NCs was reduced to half of that in neat APOL. This might be explained from eq 3, where excess H_2O shifts the equilibrium to the left in favor of CdO which could not only retard further etching but, as explained above, could also act as a passivating layer to improve PL quantum yield. Moreover, in the absence of H_2O the CdO solubilization from eq 3 is accelerated to provide the necessary H_2O for the solubilization of SeO_2, shown in eq 2. Based on this, the following model emerges: "The oxidative transformations of the Se surface sites of these NCs to acidic selenium oxide byproducts assist their etching by its gradual solubilization in the basic APOL solvent. This, however, exposes the underlying cadmium NC sites, which, in the presence of water, can form cadmium oxide/hydroxide monolayer species that provide temporal resistance to further etching". Moreover, the Cd-enriched NC surface, capped either by APOL or cadmium oxide species, provides an effective surface passivation that boosts PL quantum yield values to as high as 34 ± 7%.

To test this model we chose to closely investigate the influence of solubilized cadmium ion concentration in the etching media. An initial hint for their importance was seen when one compares the duration of plateaus I and III in the PL λ_{max} vs time graph, shown in Figure 2. Of the two plateaus, the second one (regime III) is almost twice as long in duration as the first one (regime I). This might be due to the presence of significantly higher concentrations of dissolved cadmium ions in the etching medium at later stages of etching (regime III). As argued above, these cadmium ions render further dissolution of surface-bound cadmium unfavorable (see eq 3) and thus prevent exposure of the selenium sites to the oxidizing medium, which in turn is manifested by the prolonged duration of regime III. This was verified by adding various amounts of $CdCl_2$ to the APOL/H_2O (v/v = 10/1) solutions and investigating the corresponding etching characteristics of CdSe NCs. The aqueous $CdCl_2$ solution added to APOL formed immediately a white $Cd(OH)_2$ precipitate, which upon shaking it redissolved as a $[Cd(NH_2(CH_2)_3OH)_4]^{2+}$ complex.[36,37] Figure 6 illustrates the evolution of UV/vis and PL of these CdSe NCs as a function of various initial $CdCl_2$ concentrations. To maintain a linear time scale on the *x*-axis of these graphs, the zero $CdCl_2$ concentration curve was accelerated by reducing the OD at 560 nm to 0.15 as opposed to ODs of 3.0 and 1.5 of Figure 2. According to eq 3, adding various amounts of Cd^{2+} is expected to reduce the etching rate of CdSe NCs. The introduction of $CdCl_2$ in as low as 0.005 M nearly doubles the etching duration for regime I. Progressively higher initial $CdCl_2$ concentrations further reduce etching rates. Similarly, changes in the PL fwhm (Figure 6b) for all the samples exhibit the same trend as before where minima in fwhm (below 40 nm) are associated with plateau regions in Figure 6a, and the fwhm maxima are observed when the emission peak position undergoes rapid changes. These observations indicate that the addition of Cd^{2+} ions does not change the nature of this etching process but only its rate.

Obtaining high-resolution TEM images of the etched nanocrystals is highly desirable for further clarifying this etching process. The high boiling point of APOL (ca. 170 °C) and the strong hydrogen bonding between adjacent hydroxyl and amine moieties render this solvent unsuitable for TEM characterization. That necessitated the re-exchanging of the surface capping agent from APOL to TOPO/TOP. This was achieved by adding TOPO/TOP together with *n*-octylamine solution to the APOL-capped CdSe NC solution and precipitating out the NCs in methanol. The UV/vis spectra of CdSe NCs coated with APOL show little change after the surface exchange indicates that the fast exchange process has little effects on the size and size distribution (See Figure S4 in the Supporting Information). However, when the CdSe nanocrystals are smaller than 2 nm, it is impossible to retrieve the APOL-coated CdSe nanocrystal by this surface exchange because it cannot be precipitated out by methanol after surface exchange. The TOPO/TOP/*n*-octylamine coated CdSe NCs formed aggregate-free solutions in

(34) Spanhel, L.; Haase, M.; Weller, H.; Henglein, A. *J. Am. Chem. Soc.* **1987**, *109*, 5649−5655.
(35) Kim, D.; Miyamoto, M.; Nakayama, M. *Phys. Status Solidi C* **2004**, *1*, 835−838.
(36) Zhou, J.-S.; Cai, J.; Wang, L.; Ng, S.-W. *J. Chem. Soc., Dalton Trans.* **2004**, 1493−1497.
(37) Sillen, L. G.; Martell, A. E. *Stability constants of metal-ion complexes*; The Chemical Society, Burlington House: London, 1964.

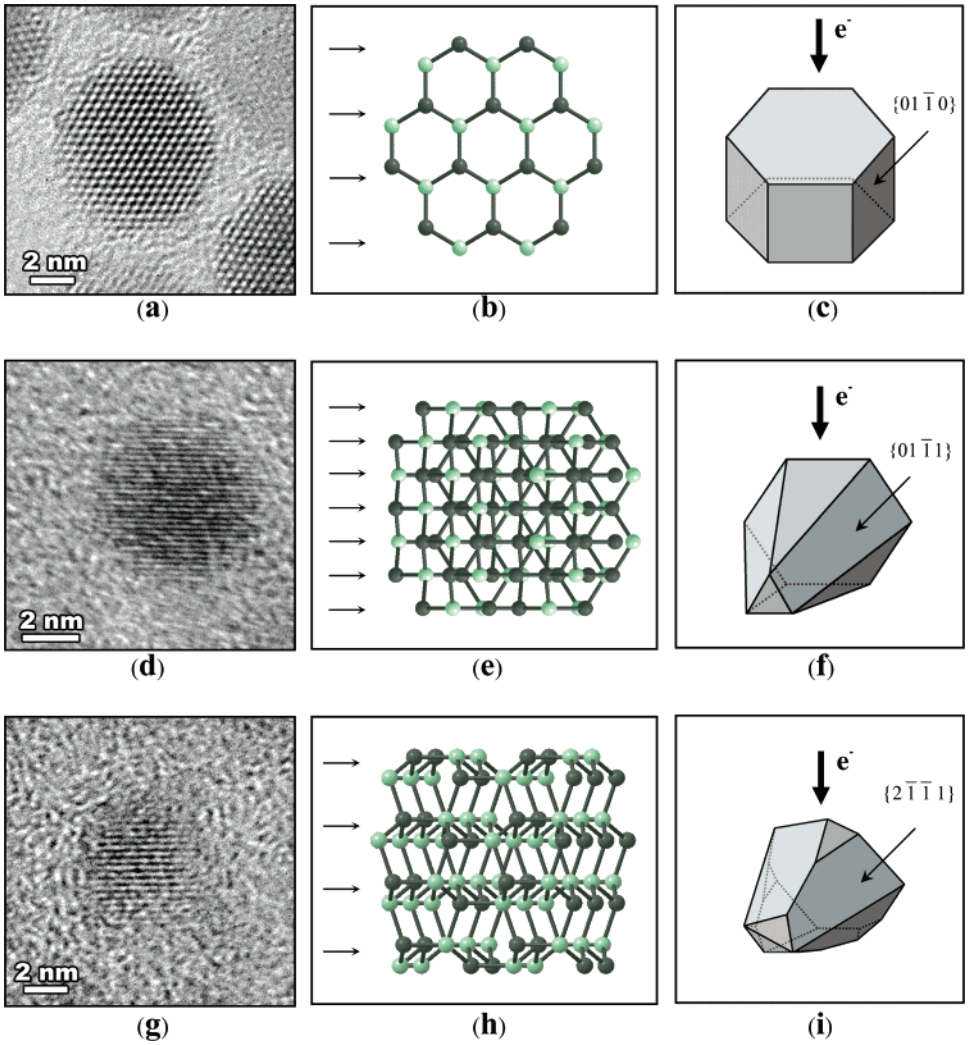

Figure 7. High-resolution TEM images of the CdSe NCs before (a) and after etching for 24 h (d) and 2 weeks (g), respectively. The ball-and-stick structures of parts b, e, and h along with the schematic diagram of NC shapes in parts c, f, and i correspond to the respective HRTEM images (see text for details).

chloroform that permitted us to deposit well-dispersed NCs onto copper-supported ultrathin carbon films for HRTEM investigation.

For microscopic investigations, slightly larger CdSe NCs were utilized to facilitate HRTEM imaging. The etching process was started with CdSe NCs having their first electronic transition peak at ca. 625 nm, PL peak at ca. 635 nm, and an average size of 6.2 ± 0.37 nm.[38] Figure 7a is a representative HRTEM image of one such particle. Our previous investigations have shown that these NCs exhibit a tabular hexagonal morphology (Figure 7c).[38] In this observation, many of these particles were hexagonal in projection and exhibited three intersecting sets of 0.37 nm lattice fringes running parallel to the edges of the particles. These fringes correspond to the $\{01\bar{1}0\}$ planes of the wurtzite structure for CdSe, and the intersecting fringe pattern observed experimentally is what one would expect for particles oriented with [0001] parallel to the beam direction. The [0001] projection of the wurtzite structure is shown in Figure 7b with one of the sets of $\{01\bar{1}0\}$ planes indicated by arrows. As discussed previously,[38] this is consistent with the NCs adopting a tabular hexagonal morphology bounded by (0001) top and bottom facets and $\{01\bar{1}0\}$ side facets (Figure 7c). The preferred orientation of these as-synthesized TOPO/TOP coated NCs and their tendency to self-assemble are partially due to the slow drying that, together with their tabular shape, forces them to adopt this unique configuration.[38]

Figure 7d is a representative HRTEM image of a CdSe NC etched for 24 h in APOL/H_2O (v/v = 10:1) at 80 ± 5 °C, shifting its PL emission from ca. 635 nm to ca. 600 nm. Prior to imaging, the NC capping agent was exchanged from APOL to TOPO/TOP/*n*-octylamine as discussed above. The mean size of these 24 h etched NCs is 5.3 ± 0.4 nm (see TEM-derived size distributions in Figure S7 of the Supporting Information). In HRTEM images obtained from these particles, only a single set of lattice fringes was observed (Figure 7d and Figure S5 of the Supporting Information), with a much finer spacing than those observed for the unetched samples (e.g., Figure 7a). In each case these fringes had a spacing of 0.21 nm which is close to the resolution limit of the instrument (<0.19 nm). This corresponds to the spacing of the $\{2\bar{1}\bar{1}0\}$ planes of CdSe with the wurtzite structure. To explain this observation, further

(38) Kang, D.; Lee, J.; Papadimitrakopoulos, F.; Aindow, M. *Philos. Mag. Lett.* **2003**, *83*, 709.

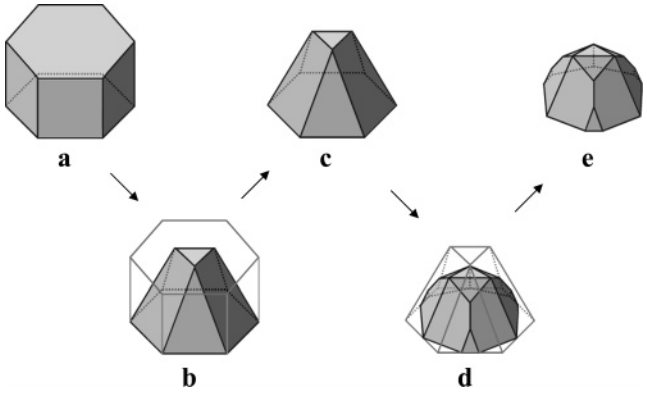

Figure 8. Schematic CdSe NC shape evolution according to the morphologies observed in Figure 7 (see text for details).

consideration was given to the characteristics of the wurtzite structure and, in particular, to that of the Cd-terminated facets.

The preferential oxidation and removal of the Se sites from the NC surface leaves behind oxide- or amine-terminated Cd-rich surfaces. Based on this, facets that are terminated solely with Cd atoms are expected to be more stable in this etching medium as opposed to those containing all Se or varying proportions of Cd and Se atoms. Because the wurtzite structure is noncentrosymmetric, the hexagonal tabular morphology of the unetched NCs (Figure 7c) exhibits Se- and Cd-terminated top and bottom (0001) planes, respectively, while the $\{01\bar{1}0\}$ side facets are stoichiometric (i.e., equal amount of Cd and Se atoms present). As shown in Figure 8a−c the preferential attack of the Se-rich planes would eventually lead to pyramidal morphologies (Figure 8c), possessing the original Cd-terminated (0001) base and six new Cd-terminated $\{01\bar{1}1\}$ facets. If such particles lay with one of their $\{01\bar{1}1\}$ facets parallel to the support film surface (as shown in Figure 7f), then for an untilted sample the beam direction would be parallel to [0 16 $\overline{16}$ 9]. In this orientation, the $(2\bar{1}\bar{1}0)$ planes would be resolvable in each NC (shown with arrows in Figure 7e), corresponding to the lattice spacing of 0.21 nm observed in Figure 7d. We note that, in the limit, we would expect this process to result in pyramidal particles with a triangular, rather than a hexagonal, Cd-terminated (0001) base. This is because the space group for the wurtzite structure is $P6_3mc$ (#186) and exhibits 3-fold, rather than 6-fold, symmetry. Although the bond configurations for the planes $(01\bar{1}1)$, $(\bar{1}011)$, and $(1\bar{1}01)$ will be different from those of $(\bar{1}101)$, $(0\bar{1}11)$, and $(10\bar{1}1)$, all six planes are Cd-terminated with the exception of three of the six facet junctions with the (0001) base forming alternating Se- and Cd-terminated edges.[39] Thus, to eliminate the Se-terminated edges, one would have to form a triangular-based pyramidal NC bounded by a Cd-terminated (0001) base and only a subset of three $\{01\bar{1}1\}$ facets (either $(\bar{1}101)$, $(0\bar{1}11)$, and $(10\bar{1}1)$ or $(01\bar{1}1)$, $(\bar{1}011)$, and $(1\bar{1}01)$ depending upon the orientation of the bases with respect to the lattice axes). Such a sharply edged triangular-based pyramidal NC configuration is considered to be less energetically favorable than the hexagonally shaped pyramidal structure shown in Figure 7f. More importantly, however, the tips of these hexagonal or trigonal pyramids expose a certain number of Se sites that increase as their apexes become less sharp. It is these sites where one would expect the point of further attack by the etching medium. For the wurtzite structure, if one removes a row of Se and Cd atoms along the six edges of the $\{01\bar{1}1\}$ family of facets (see Figures 8c−e), six new $\{2\bar{1}\bar{1}1\}$ facets are created. These facets are the next most densely packed Cd-terminated surfaces for wurtzite, and their exposure would leave fewer exposed Se sites at the apex and base edges.

This is consistent with our experimental observations. After more extended exposure to the etching medium (about two weeks), their sizes of the NCs were further reduced. The mean size of the 2 week etched NCs was 4.1 ± 0.4 nm (see TEM-derived size distributions in Figure S7 of the Supporting Information), with a PL emission of ca. 525 nm, and one example is shown in Figure 7g and Figure S6 of the Supporting Information. Here again only a single set of lattice fringes was observed in images obtained from these particles, and in each case these fringes had a spacing of 0.32 nm. This spacing corresponds to that of the $\{01\bar{1}1\}$ planes of the wurtzite structure for CdSe. One can account for this observation if the NCs were to adopt the morphology shown in Figure 8e and lay with one of their $\{2\bar{1}\bar{1}1\}$ facets parallel to the support film surface (as shown in Figure 7i). Thus, for an untilted sample the beam direction would be parallel to [32 $\overline{16}$ $\overline{16}$ 9]. In this orientation only a single set of $(10\bar{1}1)$ planes would be resolvable in each NC (shown with arrows at Figure 7h), corresponding to a lattice spacing of 0.32 nm observed experimentally (Figures 7g and S6 of the Supporting Information). Since the proposed pyramidal CdSe nanocrystals are terminated by Cd-rich facets, one might expect that the atomic composition of the CdSe will deviate from the 1:1 ratio. Energy-dispersive X-ray analysis (EDX) revealed that the Cd/Se ratio has changed from 48/52% to 59/41% (See Supporting Information Figure S8) for unetched and 2 week etched CdSe nanocrystals, respectively. As such, these HRTEM observations and EDX analysis are in accordance with the bottleneck etching behavior shown in Figures 1 and 2 and further reinforce the etching mechanism proposed above.

One issue which remains unresolved is why none of the etch NCs were aligned with the beam direction parallel to [0001]. For the pyramidal morphologies shown in Figure 8c and e, the largest facet is the Cd-terminated $(000\bar{1})$, and so one might expect a significant proportion of the etched NCs to lie with this surface parallel to the support film. Since none of the etched NCs exhibit lattice fringe patterns similar to that for the unetched NCs (e.g., Figure 7a), they cannot be adopting this orientation. One possibility is that this is due to the surfactant arrangement on the Cd-terminated $(000\bar{1})$ surface and further work is underway to test this hypothesis.

Conclusions

The gradual etching of CdSe NCs in 3-amino-1-propanol (APOL)/H_2O (v/v = 10:1) was investigated with UV−visible and photoluminescence (PL) spectroscopy and high-resolution transmission electron microscopy (HRTEM). The observed blue shifts of the UV/vis absorption and PL emission spectra were found to exhibit a characteristic bottleneck behavior that was ascribed to the formation of Cd-terminated facets that temporally impede etching. Based on a comprehensive study of the effects of (i) oxygen, (ii) H_2O, and (iii) Cd^{2+} ion concentrations in the etching medium, the following mechanism is proposed. The exposed Se sites on the CdSe surface is oxidized by oxygen to

(39) Cd or Se atoms connected to less than two nearest neighbors (Se or Cd respectively) are considered unstable and not part of the NC structure presently discussed.

acidic SeO_x byproducts, which are readily dissolved in APOL, exposing the underlying Cd-sites that, upon coordination with both amines and hydroxyl moieties, temporally impede NC dissolution. As indicated by HRTEM investigations, the preferential alignment of etched CdSe NCs along the Cd-terminated $\{01\bar{1}1\}$ and $\{2\bar{1}\bar{1}1\}$ facets further supports the proposed etching mechanism. The novel ability of this method to selectively yield Cd-terminated facets may find unique applications in the engineering of more precisely defined CdSe quantum-confined geometries.

Acknowledgment. The authors would like to thank Dr. James R. Knox and Jack Gromek for the helpful discussions on the XRD experiment. Partial support from ONR (Grant No. N00014210883), BMDO (Grant No. N00178-98-C-3035), and the Critical Technology Program (Grant No. 98CT025) is greatly appreciated.

Supporting Information Available: ^{1}H NMR spectra of TOPO/TOP/hexadecylamine capped CdSe nanocrystals, APOL-exchanged CdSe nanocrystals, and TOPO/TOP/*n*-octylamine re-exchanged CdSe nanocrystals; comparative UV/vis spectra of APOL- and TOPO/TOP/*n*-octylamine-coated CdSe NCs; low magnification TEM images and size distribution analysis histogram; Additional HRTEM images of etched CdSe nanocrystals; Energy-dispersive X-ray analysis of the CdSe nanocrystals before and after etching are provided. This material is available free of charge via the Internet at http://pubs.acs.org.

JA0465404